# Clusters of circulating tumor cells traverse capillary-sized vessels

Sam H. Au[a,b], Brian D. Storey[c], John C. Moore[d,e,f], Qin Tang[d,e,f], Yeng-Long Chen[g], Sarah Javaid[d,h], A. Fatih Sarioglu[a,b], Ryan Sullivan[d,h], Marissa W. Madden[d], Ryan O'Keefe[d], Daniel A. Haber[d,h,i], Shyamala Maheswaran[b,d], David M. Langenau[d,e,f], Shannon L. Stott[a,d,h,1], and Mehmet Toner[a,b,j,1]

[a]Center for Engineering in Medicine, Massachusetts General Hospital, Harvard Medical School, Boston, MA 02114; [b]Department of Surgery, Massachusetts General Hospital, Harvard Medical School, Boston, MA 02114; [c]Olin College, Needham, MA 02492; [d]Massachusetts General Hospital Cancer Center, Harvard Medical School, Charlestown, MA 02129; [e]Department of Molecular Pathology and Regenerative Medicine, Massachusetts General Hospital, Charlestown, MA 02129; [f]Harvard Stem Cell Institute, Cambridge, MA 02138; [g]Institute of Physics, Academia Sinica, Taipei 11529, Taiwan; [h]Department of Medicine, Massachusetts General Hospital, Harvard Medical School, Boston, MA 02114; [i]Howard Hughes Medical Institute, Bethesda, MD 20815; and [j]Shriners Hospital for Children, Boston, MA 02114

Edited by Konstantinos Konstantopoulos, The Johns Hopkins University, Baltimore, MD, and accepted by the Editorial Board February 26, 2016 (received for review December 12, 2015)

**Multicellular aggregates of circulating tumor cells (CTC clusters) are potent initiators of distant organ metastasis. However, it is currently assumed that CTC clusters are too large to pass through narrow vessels to reach these organs. Here, we present evidence that challenges this assumption through the use of microfluidic devices designed to mimic human capillary constrictions and CTC clusters obtained from patient and cancer cell origins. Over 90% of clusters containing up to 20 cells successfully traversed 5- to 10-μm constrictions even in whole blood. Clusters rapidly and reversibly reorganized into single-file chain-like geometries that substantially reduced their hydrodynamic resistances. Xenotransplantation of human CTC clusters into zebrafish showed similar reorganization and transit through capillary-sized vessels in vivo. Preliminary experiments demonstrated that clusters could be disrupted during transit using drugs that affected cellular interaction energies. These findings suggest that CTC clusters may contribute a greater role to tumor dissemination than previously believed and may point to strategies for combating CTC cluster-initiated metastasis.**

microfluidics | cancer metastasis | CTC clusters | circulating tumor cell cluster microemboli | capillary microhemodynamics

Circulating tumor cells (CTCs) drive metastasis by disseminating from primary tumors to seed metastases in distant organs. These rare cells may serve as prognostic/predictive cancer markers or may help identify potential therapeutic targets (1–5). However, individual "singlet" CTCs may not be the strongest initiators of secondary tumors. Aggregates containing two or more CTCs (also known as circulating tumor microemboli; herein, CTC clusters) have been known for decades to seed colonies with greater efficiencies than individual CTCs (6–8). Recent data suggest that clusters may have 50 times greater metastatic potential than individual CTCs (9). The greater colonization efficiency of CTC clusters may be due to a number of factors including protection against anchorage-dependent apoptosis (5, 10), the cooperation of heterogeneous cell phenotypes within CTC clusters (11), and shielding from assault by immune cells (2, 12). Beyond their role in metastasis, CTC clusters may also serve as biomarkers for early detection (13), as prognostic markers (5, 9), and may have utility for noninvasively tracking changing drug susceptibilities in patients undergoing treatment (14).

Despite their biological significance, the behavior of CTC clusters in circulation is largely unexplored (3, 15). The current consensus is that CTC clusters are incapable of transiting through capillaries because of their large size and therefore immediately arrest in circulation, leading to the rupture of vessel walls (2, 4, 15). This idea has remained unchallenged for decades (16), despite the fact that many groups have reported the isolation of CTC clusters, sometimes containing up to 100 cells, from the peripheral blood of cancer patients (2, 5, 9–11, 17–19). Since blood is routinely drawn from the venous circulation of the arm, it is unlikely that CTC clusters could be consistently collected unless they passed through both pulmonary capillary beds and finger capillaries at least once. Furthermore, CTC clusters have been shown in animal models to exhibit circulating half-lives on the order of minutes (9) and to seed metastases in distant organs (20). Taken together, these observations suggest that CTC clusters may possess the ability to traverse small vessels (Fig. 1*A*).

In this work, microfluidic constriction devices were engineered with dimensions mimicking human capillaries to study the behavior of CTC clusters within constrictions under physiological temperature and pressures. Although not perfect analogs of human capillaries, microchannel constrictions are advantageous for studying CTC cluster behavior for a number of reasons: (*i*) devices can be easily integrated with imaging systems permitting sensitive multifluorescence analyses of cellular responses in real time; (*ii*) unlike larger blood vessels, which are suitably modeled as tubes within fluids, the mechanical properties of capillaries are better modeled as tunnels within elastic solids (21); (*iii*) similar to other blood cells (22), physical parameters such as pressure, constriction size, cell elasticity, cell size, and strengths of intercellular adhesions likely dominate the transit behavior of CTC clusters in circulation. Many of these parameters can be precisely controlled in microfluidic

## Significance

Metastasis is responsible for 90% of cancer-related deaths and is driven by tumor cells circulating in blood. However, it is believed that only individual tumor cells can reach distant organs because multicellular clusters are too large to pass through narrow capillaries. Here, we collected evidence by examining clusters in microscale devices, computational simulations, and animals, which suggest that this assumption is incorrect, and that clusters may transit through capillaries by unfolding into single-file chains. This previously unidentified cell behavior may explain why previous experiments reported that clusters were more efficient at seeding metastases than equal numbers of single tumor cells, and has led to a strategy that, if applied clinically, may reduce the incidence of metastasis in patients.

Author contributions: S.H.A., B.D.S., J.C.M., Q.T., D.A.H., S.M., D.M.L., S.L.S., and M.T. designed research; S.H.A., B.D.S., J.C.M., Q.T., Y.-L.C., S.J., R.S., M.W.M., and R.O. performed research; S.H.A., B.D.S., J.C.M., Q.T., Y.-L.C., S.J., and A.F.S. contributed new reagents/analytic tools; S.H.A., B.D.S., J.C.M., Q.T., S.L.S., and M.T. analyzed data; and S.H.A. wrote the paper.

The authors declare no conflict of interest.

This article is a PNAS Direct Submission. K.K. is a guest editor invited by the Editorial Board.

Freely available online through the PNAS open access option.

[1]To whom correspondence may be addressed. Email: mehmet_toner@hms.harvard.edu or sstott@mgh.harvard.edu.

This article contains supporting information online at www.pnas.org/lookup/suppl/doi:10.1073/pnas.1524448113/-/DCSupplemental.

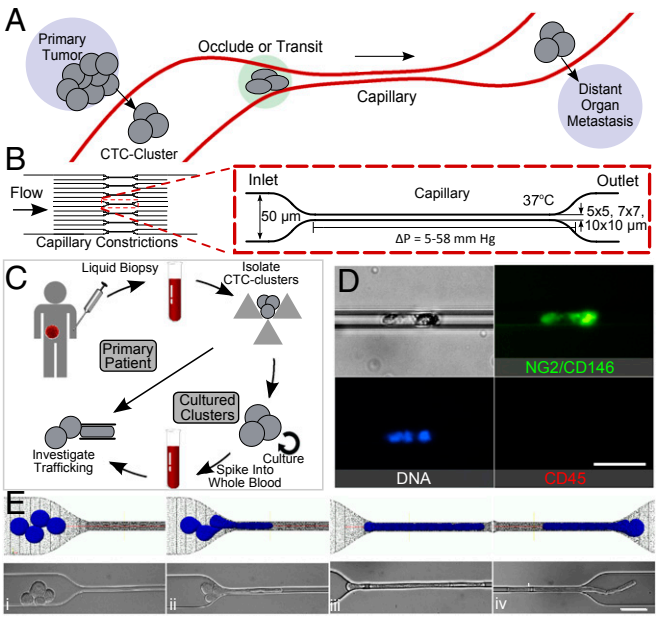


**Fig. 1.** (*A*) Diagram of CTC clusters occluding or transiting through capillary to seed metastases. (*B*) Microfluidic device schematic, 16 parallel microchannels of 5 × 5, 7 × 7, or 10 × 10-μm square cross-sections, designed to mimic capillary flow conditions (not to scale). (*C*) Experimental workflow: CTC clusters were isolated from breast or melanoma patient liquid biopsies (30). Patient clusters introduced into capillary devices directly or after ex vivo culture and spiking into whole blood. (*D*) Primary patient CTC cluster isolated from melanoma patient transiting through 10-μm capillary constriction under 7 cm $H_2O$ at 37 °C. (*E*) Computational simulation (*Top*) and micrographs (*Bottom*) of four-cell LNCaP cluster in transit: (*i*) approach, (*ii*) unfold/elongate, (*iii*) travel, (*iv*) exit/reform through a 5-μm capillary constriction. (Scale bars: 50 μm.)

systems, and (*iv*) microfluidic constrictions of this sort have previously demonstrated utility in exploring various biophysical cellular properties such as the viscoelastic properties of cancer cells (23) and neutrophils (24), examining nuclear deformability during migration (25, 26) and for phenotypic discrimination (27). Although clusters have been demonstrated to transit through 50- to 300-μm microchannels (28), capillary-sized microfluidic constrictions have yet to be studied. Observations of CTC clusters in microchannel constrictions in conjunction and in vivo models organisms reveal how CTC clusters dynamically reorganize to pass through narrow blood vessels.

## Results

Microfluidic devices designed to mimic the hydrodynamic properties of capillary networks were developed consisting of 16 parallel microchannels that taper into 5-, 7-, or 10-μm "capillary constrictions" (Fig. 1*B*). Cancer cell clusters and CTC clusters traveling through these capillary constrictions at 37 °C under physiological pressures of 7–33 cm $H_2O$ (29) were examined. Under these conditions, red blood cells assumed morphologies similar to those reported in human capillaries (*Supporting Information* and Movies S1 and S2). Transit under greater than physiological (83 cm $H_2O$) pressures is presented in the *Supporting Information*.

**CTC Clusters Transit Through Narrow Constrictions in Single File.** Primary patient CTC clusters were isolated from blood specimens of malignant melanoma patients undergoing treatment at Massachusetts General Hospital Cancer Center (Fig. 1*C*). Blood samples from 10 different patients were processed using a recently developed label-free microfluidic CTC cluster isolation technology (30). Patient CTC clusters were successfully isolated from two samples, and one CTC cluster isolated from patient MEL-142 was successfully released from the cluster isolation chip and transferred to the microfluidic capillary constriction device. Fig. 1*D* and Movie S3 depict the successful transit of this CTC cluster through a capillary constriction. This preliminary result prompted us to conduct further experiments to determine how CTC clusters could be capable of this behavior. Because of the difficulty in isolating, staining, and manipulating extremely scarce primary patient clusters, we conducted experiments using clusters from more readily available breast cancer patient cultured CTCs (Fig. 1*C*) and cancer cell lines.

Over 90% of observed cancer cell line and cultured CTC clusters, including those containing 20 or more cells (Movies S4–S6), transited through constrictions as small as 5 μm. Individual cells experienced two distinct transit phases: an entry phase where cells encountering capillary constrictions deformed and elongated (Fig. 1*Eii*) and a travel phase where cells no longer deformed but traveled at constant velocity (Fig. 1*Eiii*). These phases are consistent with the previously reported transit behaviors of individual cancer cells (23). The transit of CTC clusters incorporated these behaviors at the level of individual cells, but with added complexity due to multicellular organization (Movie S4). When entering constrictions, clusters "unfolded" so that cells could enter and pass sequentially (Fig. 1*E ii* and *iii*). After exiting constrictions, cells retracted into rounded morphologies and clusters reformed into "typical" organizations (Fig. 1*Eiv*). To determine whether cells within CTC clusters transited in single file, clusters containing mixed populations of breast cancer cells engineered to express either GFP or mCherry (in approximately equal numbers) were imaged while traversing capillary constrictions (Fig. 2*A*). Both cell bodies and nuclei traversed in single file (Fig. 2*A*). Clusters also successfully transited in similar chain-like organizations through human endothelial cell-coated microchannels (Fig. S1 and Movie S7). However, because of the variability in constriction diameters across the lengths of cellularized microchannels (Fig. S1), hydrodynamic analyses of CTC cluster transit, described below, were conducted in non–cell-coated devices.

**Single-File Transit Is Favored at Physiological Interaction Energies.** It was hypothesized that biophysical interactions between cells were responsible for rearrangement into stable single-file chains. Therefore, we developed a hybrid Brownian dynamics–Lattice Boltzmann fluid–structure interaction computational model (31) to simulate CTC cluster transit under the same conditions as the experiments described above (Fig. 2*B*). The strengths of cell–cell interactions were found to dramatically influence the transit behaviors of CTC clusters. When interaction energies were set to (*i*) $1.5 \times 10^{-3}$ J/m$^2$, to approximate experimentally published values of cell–cell adhesions in cancer cells (32, 33), simulated clusters elongated and transited in single file similar to experimentally observed clusters (Fig. 2*B*, middle row, and Movie S8); (*ii*) $6.0 \times 10^{-4}$ J/m$^2$, below physiologically relevant levels, clusters dissociated into individual cells during transit (Fig. 2*B*, bottom row, and Movie S9); and (*iii*) $7.5 \times 10^{-3}$ J/m$^2$, above physiological levels, clusters occluded constrictions (Fig. 2*B*, top row, and Movie S10). These results suggest that the reorganization of clusters into single-file chains during transit is biophysically favored at physiological cell interaction energies and that modifying these interactions may dramatically alter the fate of CTC clusters at capillary constrictions (explored below).

We next examined clusters as they transitioned from typical cluster morphologies to single-file chains of cells by observing stained cell membranes. Clusters underwent substantial reorientation as they entered constrictions (Fig. 2 *C–F* and Movies S5 and S6). Cells near the leading edges of clusters underwent less rotation than cells near the trailing edges, which often rotated 180° or more (Fig. 2*D*). This behavior suggests that cells within clusters rotated to accommodate stable intercellular junctions (Fig. 2*C*) and is consistent with computational simulations of cells demonstrating that physiological-level interaction energies result in selective cleavage and retention of specific cell–cell adhesions. Another observation was that the order in which cells transited could not be predicted by their relative distances to the constrictions before entering (Fig. 2*F*). This led us to hypothesize that the relative adhesive strengths among cells within a given cluster dictate the order in which cells reorganize to pass through

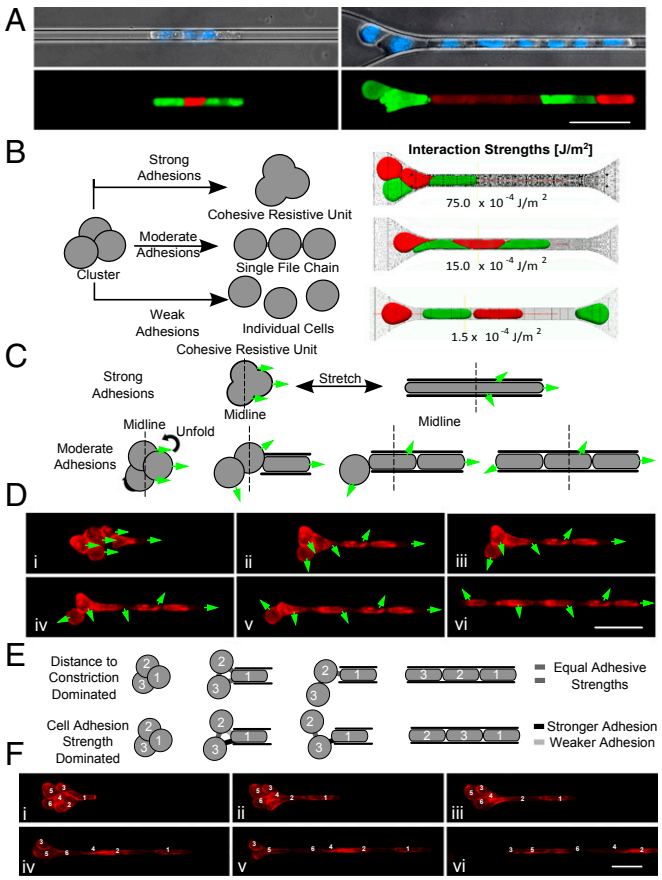


**Fig. 2.** Cluster organization. (*A*) Micrographs of three-cell (left) and eight-cell (right) MDA-MB-231 GFP or mCherry tagged cells in clusters stained with Hoechst 33342 transiting through 5-μm capillary constriction. (*B*) Conceptual cluster behavior (left) and computational transit simulations (right). Strong intercellular adhesions ($75.0 \times 10^{-4}$ J/m$^2$)—cluster occludes; moderate adhesions ($15.0 \times 10^{-4}$ J/m$^2$)—single-file transit; weak adhesions ($1.5 \times 10^{-4}$ J/m$^2$)—dissociation. (*C*) Conceptual responses: strong adhesions—minimal cell rotation; moderate adhesions—unfolding and cellular rotation. Greens arrows indicate leading edges of cells in the flow direction in frame *i*. (*D*) Time-lapse images of six-cell LNCaP cluster membrane stained with CellMask DeepRed. (*E*) Conceptual transit depends on distance to constriction (equal strength adhesions) or somewhat independent (heterogeneous adhesions). (*F*) Time-lapse images of six-cell LNCaP cluster demonstrating transit order. Cells numbered by distance to constriction in frame *i*. Experiments were conducted under 33 cm $H_2O$ at 37 °C. (Scale bars: 50 μm.)

(Fig. 2*E*). If cells must break intercellular adhesions with all cells except two adjacent neighbors, it is likely only the strongest cell–cell adhesions are retained.

**Cluster Reorganization Permits Transit by Reducing Resistance.** Inspection of CTC clusters revealed qualitative characteristics of cell reorganization during transit (above). However, the key to understanding the mechanisms that dominate cluster transit is to evaluate transit hydrodynamics. We therefore compared the transit behaviors of singlet CTCs and CTC clusters traversing 5-, 7-, and 10-μm capillary constrictions at 37 °C under 7- to 80-cm $H_2O$ applied pressures. Cell diameter(s) and transit velocities of single cell and cluster events were computed using custom Matlab scripts (Fig. 3*A* and Movie S11).

First, the velocities of singlet MDA-MB-231-LM2 cells (solid symbols) transiting under 33-cm $H_2O$ pressures through 5-μm ($n$ = 18), 7-μm ($n$ = 23), and 10-μm ($n$ = 52) constrictions were plotted vs. the ratio of cells to constriction sizes (Fig. 3 *B* and *C*). Cell velocities ranged from 5 μm/s to unrestricted fluid velocities of ~2,850 μm/s, which encompassed the physiological capillary velocity of ~200 μm/s. Singlets exhibited three distinct transit regimes dictated by relative size of the cell to the constriction (Fig. 3 *B* and *C*, solid symbols). (*i*) Small cells ($D_{cell}/D_{capillary} < 1.5$) transited at unrestricted fluid velocities. (*ii*) Large cells ($D_{cell}/D_{capillary} > 3.6$) occluded capillary constrictions (the mean ratio for occluding cells was 3.8 ± 0.5 [95% confidence interval (CI)]; occlusions occurred almost exclusively in 5-μm constrictions) and were not included in this analysis. (*iii*) Moderately sized cells ($1.5 \leq D_{cell}/D_{capillary} \leq 3.6$) transited according to a power law relation (23) with a power law exponent of −5.7 ± 0.6 (95% CI). This is consistent with theoretical scaling analyses (*Supporting Information*) and previously reported values, which suggest a power law exponent of approximately −5 (23). The strong power relation between size and velocity means that small changes in individual cell sizes dramatically affect hydrodynamic resistance (Fig. 2*A*).

The transit behavior of clusters was then investigated by overlaying cluster data points onto singlet data. The effective hydrodynamic diameters of clusters were calculated in two manners for comparison. When effective cluster diameters were set equal to spheres of equivalent volumes as all constituent cells, cluster velocities deviated significantly from singlet velocities (Fig. 3*C*) (power law exponents of −3.3 ± 0.9 vs. −5.7 ± 0.6, 95% CI), indicating that clusters did not act as cohesive resistive units. However, when cluster diameters were assumed to equal the diameters of their largest constituent cells, the transit of CTC clusters was statistically indistinguishably from singlet counterparts (Fig. 3*B*) (power law exponents, −4.7 ± 1.2 vs. −5.7 ± 0.6, 95% CI). This agreement suggests that the resistances of examined clusters were dominated by the largest cell within each cluster; a result consistent with the singlet cell findings that transit velocities depended strongly on size (above). It should be noted that this approximation was accurate for clusters containing relatively few cells (less than five in most cases). In the general case, the behavior of clusters in constrictions was better approximated as the sum of the resistances of each individual cell in the cluster (*Supporting Information* and Fig. S2). Detailed hydrodynamic analyses of CTC cluster transit using an expanded dataset with transit scaling analyses are included in the *Supporting Information* and Figs. S2–S4. Clusters that passed through constrictions were observed to return to spherical morphologies and reassemble into typical "cluster" morphologies within seconds (*Supporting Information*, Fig. S5, and Movie S12). Transited clusters also remained viable after exiting constrictions (Fig. S5) and proliferated at rates indistinguishable from controls (Fig. S6). Theoretical cell and cluster resistances derived from hydrodynamic analyses are presented for comparison in Fig. S7.

**Cell Nuclei Contribute Resistance in Very Narrow Vessels.** To investigate the role of nuclei in cluster transit, the sizes and velocities of nuclei within singlets and clusters were analyzed as described above. Nuclei deformed from rounded to elongated ellipsoidal morphologies upon entering constrictions (Fig. 3*D* and Movie S13). The dependence of nuclear size on transit behavior is plotted in Fig. 3*E*. In 10-μm channels ($n$ = 14), cell nuclei traversed capillaries at unrestricted fluid velocities similar to whole-cell studies (Fig. 3 *B* and *C*). In 7-μm channels ($n$ = 29), nuclear diameters were not correlated with cell velocities, suggesting that nuclei were not large enough to offer significant resistance. However, in 5-μm channels, nuclei in both singlets/clusters ($n$ = 35/13, respectively) were inversely correlated with cell velocities and were statistically indistinguishable from one another (power law exponents, −4.3 ± 1.6 vs. −3.2 ± 2.2, respectively, 95% CI).

Interestingly, the diameter-to-constriction ratios that dictated transit regimes for whole cells (Fig. 3 *B* and *C*) (above) also appeared to be valid for nuclei-to-constriction ratios. Nuclei traversing 5-μm constrictions had diameter ratios within the power law regime calculated for whole cells ($1.7 \leq D_{nucleus}/D_{capillary} \leq 2.5$) but below the whole-cell power law regime for most cells in 7-μm constrictions ($1.2 \leq D_{nucleus}/D_{capillary} \leq 1.8$) and all nuclei in 10-μm constrictions ($0.9 \leq D_{nucleus}/D_{capillary} \leq 1.3$). These findings suggest that nuclei may play a role in the transit of CTCs and CTC clusters in narrow (~5 μm) but not larger capillaries.

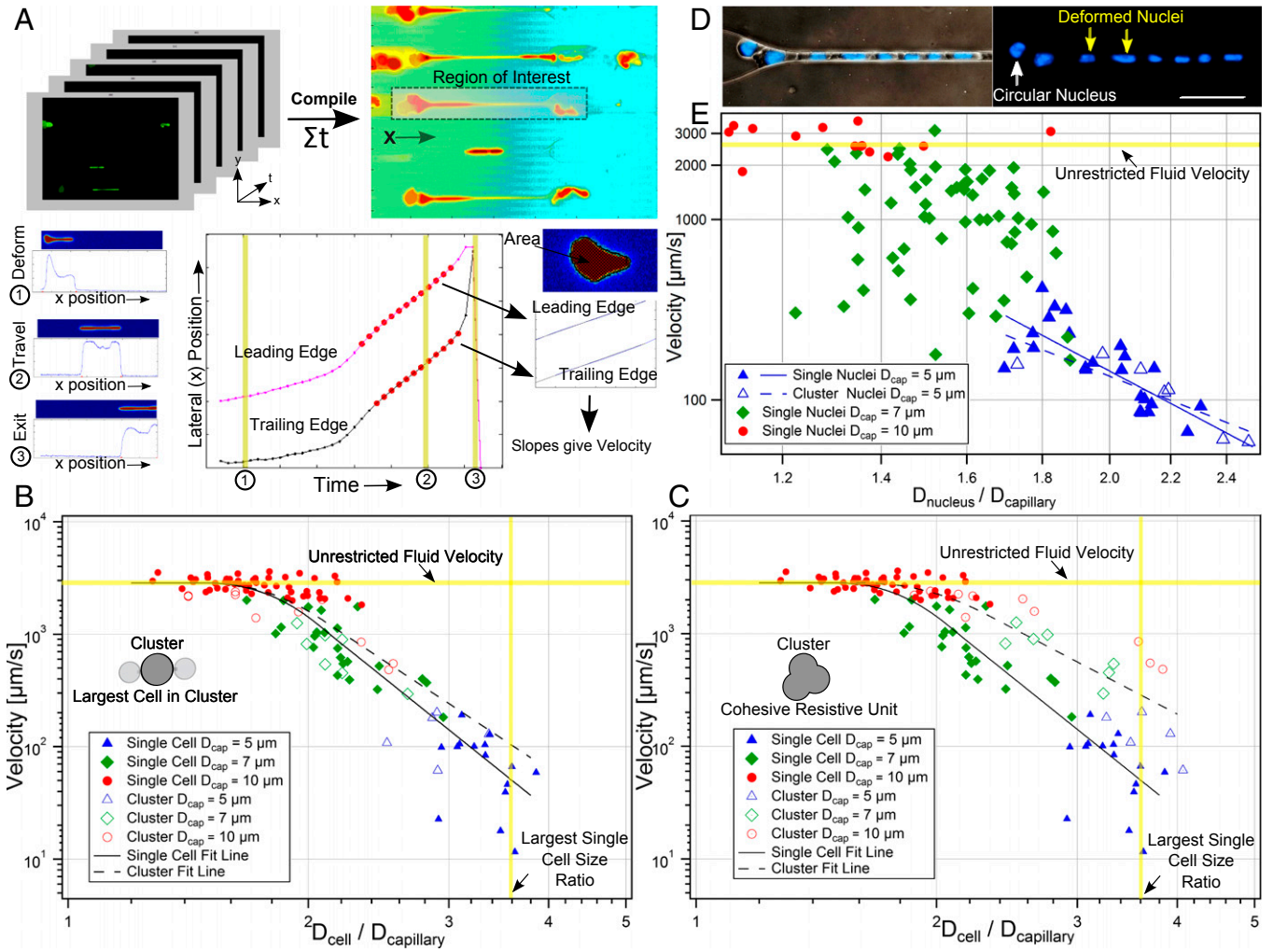


**Fig. 3.** Hydrodynamic analysis. (*A*) Size and velocity determination. (*B* and *C*) Velocities of singlet MDA-MB-231 cells traversing 5-μm (blue triangle, $n = 18$), 7-μm (green diamond, $n = 23$) or 10-μm (red circle, $n = 52$) microchannels vs. the ratios of cell-to-constriction diameters ($D_{cell}/D_{capillary}$). Cells exhibited three transit regimes: $D_{cell}/D_{capillary} < 1.5$—unrestricted fluid velocity; $D_{cell}/D_{capillary} > 3.6$—cells occluded; $1.5 \leq D_{cell}/D_{capillary} \leq 3.6$—transit under power law relation. Clustered MDA-MB-231 cells plotted assuming (*B*) cluster sizes equivalent to largest constituent cells or (*C*) cell volumes summed. Clusters match the color/shape of individual cells (above) but are hollow ($n = 5, 7, 10$, respectively). Single cells (solid lines) and clusters (dashed lines) were best fit to log-log transformed data. (*D*) Micrographs of eight-cell Hoechst 33342 stained MDA-MB-231 cluster in 5-μm capillary constrictions. Nuclei changed from circular (white arrow) to elongated (yellow arrows) upon entering. (Scale bar: 50 μm.) (*E*) MDA-MB-231 nuclear velocity vs. ratio of nuclear diameter to constriction size for single cells traversing 5-μm ($n = 23$), 7-μm ($n = 59$) and 10-μm ($n = 14$) capillary constrictions. Clusters traversing 5-μm constrictions ($n = 6$) were plotted as their largest constituent nuclei.

**Human CTC Clusters Transit in Whole Blood.** Cultured CTC clusters were derived from four breast cancer patients undergoing treatment at Massachusetts General Hospital and cultured as previously described (14). Cultured CTC clusters were spiked into whole blood before introduction into capillary constriction devices to better mimic the properties of the vascular fluid environment (Fig. 1*C*). Cultured human CTC clusters traversed constrictions in the same single-file manner as cancer cell and primary patient clusters (Fig. 4*A* and Movie S12). Importantly, cultured CTC clusters were grown as 3D aggregates in suspension and were handled without chemical or enzymatic agents that may have interfered with cell–cell adhesions. The hydrodynamic behavior of cultured CTC clusters and singlets from one patient (Brx-50) exhibited similar inverse relationships to cell size as cancer cells tested above (Fig. 4*B*) (power law exponents, $-3.89 \pm 1.5$ and $-4.0 \pm 1.8$, $s^{-1}$, 95% CI, respectively). Using the largest cell in each cluster as the effective cluster size (as described above), cluster velocities were slightly but significantly lower than singlet velocities ($P < 0.05$). It is unclear why this is the case, although interactions of CTCs and red blood cells within the capillary constrictions may have been a contributing factor (Fig. 4*Ai–iii*).

**Drugs Disrupt Clusters in Transit.** Computational simulations suggested that weakening cell–cell interaction energies could dissociate clusters in transit (Fig. 2*B*). To test this hypothesis, Brx-50 patient cultured CTC clusters were treated with 0.1, 1.0, or 10.0 μM FAK inhibitor 14 (FAK I-14), a selective small molecular inhibitor of focal adhesion kinase (involved in cell–matrix adhesions) up-regulated in many tumors (34) or paclitaxel (PTX), a commonly used chemotherapeutic agent that has been shown to weaken cell–cell adhesions (35), for 24 h before transit through 7-μm capillary constrictions at 20 cm $H_2O$. None of the drug-treated clusters were observed to undergo significant dissociation or loss of viability vs. vehicle controls before introduction into capillary constriction devices, suggesting that, although these compounds are known to induce apoptosis, that programmed cell death was not primarily responsible for observed effects. After entering capillary constrictions, drug-treated clusters were disrupted into singlets and smaller aggregates (Fig. 4*C* and Movie S14) in a similar manner predicted by computational simulations (Fig. 2*B*). Cultured CTC clusters treated with 1.0 μM or greater FAK I-14 or PTX showed statistically significantly greater probabilities of disruption vs. control clusters (FAK I-14: 1.0 μM, 18.1 ± 4.9%, $P < 0.05$; 10.0 μM,

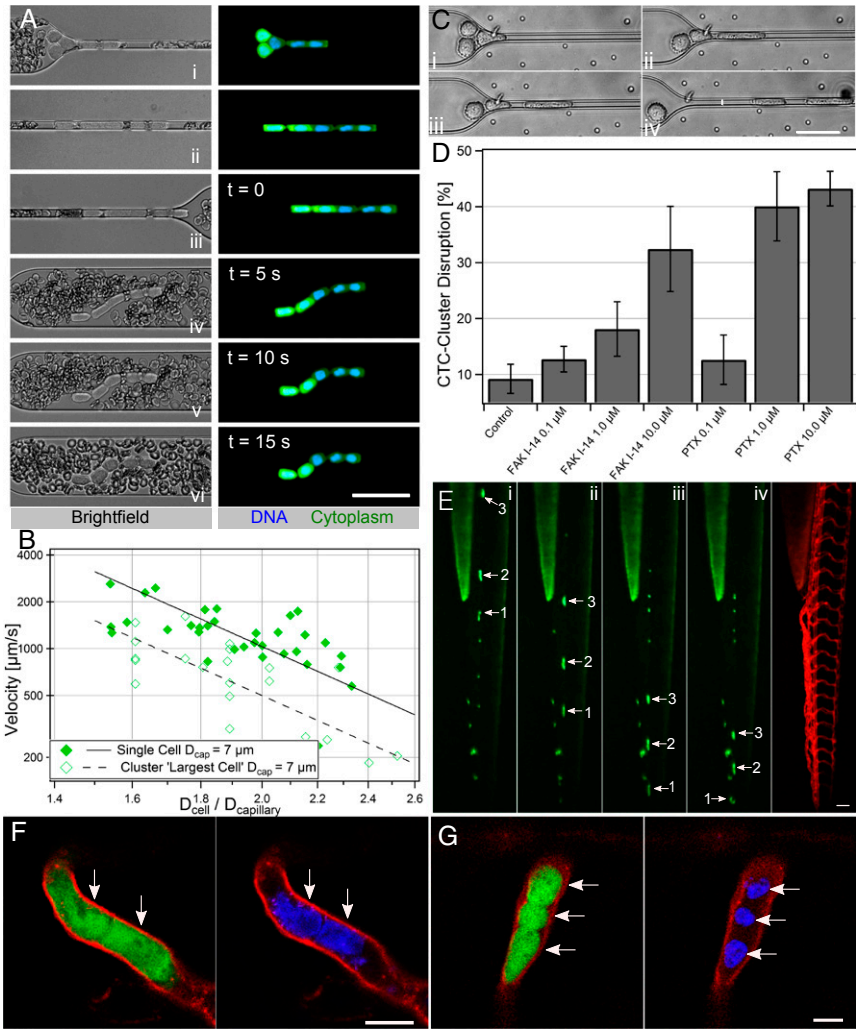


**Fig. 4.** Transit, disruption, and transplantation of cultured CTC clusters. (*A*) Micrographs of Hoechst 33342 stained, GFP tagged breast cancer patient cultured CTC clusters (BRx-50) surrounded by red blood cells in whole blood traversing 7-μm capillary constriction under 20 cm $H_2O$ (Left) bright-field and (Right) nuclear and cytoplasmic. Time stamps for *iii–vi* show recovery after exit. (*B*) Plot of velocities vs. diameter ratios of individual (diamonds, $n = 33$) and cultured CTC clusters (hollow diamonds, $n = 22$) assuming largest cell represents cluster resistance. (*C*) Time-lapse sequence of three-cell Brx-50 cluster treated with 10.0 μM focal adhesion kinase inhibitor 14 dissociating into single cells within 7-μm channel at 20 cm $H_2O$. (*D*) Constriction disruption efficiency of Brx-50 clusters preincubated with 0.1, 1.0, or 10 μM focal adhesion kinase inhibitor 14 (FAK I-14) or paclitaxel (PTX) for 24 h vs. vehicle controls. At least three device replicates were conducted per case with 15 or more clusters per replicate. (*E*) Time-lapse images (Left) showing transplanted Brx-50 cluster transiting through dorsal aorta of 3-d postfertilization *Tg (kdrl:mCherry)* zebrafish with fluorescently labeled vasculature of a different, but representative, animal (right). Numbers and arrows indicate three clusters in transit; cluster 1 transitions from dorsal aorta to caudal vein in frame *iv*. (*F* and *G*) Cytoplasmic (*Left*) and nuclear (*Right*) stained Brx-50 clusters in single file: (*F*) two-cell cluster in mandibular arch vessel and (*G*) three-cell cluster in intersegmental vessel (arrows indicate distinct cells or nuclei). (Scale bars: 50 μm in frames *A*, *C*, and *E*; 10 μm in frames *F* and *G*.)

32.4 ± 7.6%, $P < 0.0001$; PTX: 1.0 μM, 40.1 ± 6.2%, $P < 0.0001$; 10.0 μM, 43.2 ± 3.1%, $P < 0.0001$, vs. control, 9.2 ± 2.6%) (Fig. 4*D*).

**CTC Clusters Transit Through Capillary-Sized Vessels.** To explore the behavior of CTC clusters in capillary-sized vessels, cultured human CTC clusters (Brx-50) tagged with GFP and nuclear stained with Hoechst 33342 were transplanted into the circulation of *Tg(kdrl:mCherry)* transgenic zebrafish embryos 3 days postfertilization. Over 120 CTC clusters transplanted into the circulation of 51 independent animals were observed to transit through the comparatively wider dorsal aortas and caudal veins (Fig. 4*E* and Movie S15) as well as narrower vessels such as the aortic arches (Movie S16), branchial arches (Movie S16), mandibular arches (Fig. 4*F*), and intersegmental vessels (Fig. 4*G* and Movie S17). Because individual zebrafish vessels, unlike engineered microfluidic constrictions, vary greatly in diameter (36) and cannot be practically set to desired intravascular pressures, cluster velocities in zebrafish could not be directly compared with those within capillary constrictions. However, CTC clusters remained viable (as determined by membrane impermeable fluorescent molecule localization) and exhibited similar single-file reorganization behavior as in vitro counterparts (Fig. 4 *F* and *G*).

An interesting observation was that many CTC clusters that entered the dorsal aorta were observed to deposit in the caudal vein plexus (Fig. S8), directly upstream of a sharp 180° turn in the circulation where the dorsal aorta feeds into the caudal vein, a geometry not present in human capillaries. In addition, CTC clusters that appeared to have stopped within the vasculature were observed to have transited from apparent occlusion sites over minutes to hours (Fig. S9), suggesting the potential for reinitiation of cluster transit after occlusion and/or a slow "creeping" transit behavior. This observation may explain the reportedly short circulating half-lives of CTCs (37) and CTC clusters (9) because increased residence times within capillaries may inhibit/delay their detection or sampling from larger vessels. Further studies are needed to explore these phenomena.

## Discussion

In contradiction to the decades-held assumption that CTC clusters are incapable of transiting through narrow vessels (16), this work is to our knowledge the first direct evidence that CTC clusters can traverse capillary-sized constrictions and blood vessels under physiological conditions. Even in whole blood, cultured CTC clusters successfully transited through capillary constrictions with over 90% efficiency. Clusters of both mesenchymal (cultured breast cancer and MDA-MB-231) and epithelial (primary melanoma patient and LNCaP) cell phenotypes exhibited similar transit behaviors. These results are supported by both computational simulations, which verified that this behavior was favored at physiological cell–cell interaction energies, and by in vivo xenotransplantation studies. Zebrafish embryos were chosen as model organisms for transplantation because they have ∼5- to 10-μm-diameter one-cell-thick blood vessels that are close analogs of human capillaries (36), have conservative pressure drops across their circulation [∼10–100 times lower than that across human capillaries (29, 38)], and, unlike mouse or rat models, are optically transparent allowing for whole-organism imaging of transgenically labeled vasculature. The remarkable ability of CTC clusters to transit

through capillary-sized vessels suggests that the term circulating tumor "microemboli" may be a misnomer and that the dissemination of CTC clusters to distant organs may contribute to their greater metastatic potential.

The key to CTC cluster transit through narrow blood vessels appears to be their ability to rapidly and reversibly unfold into single-file chains through selective cleavage of intercellular adhesions. This unfolding behavior is critically important for successful transit because, instead of acting as cohesive resistive units, CTC clusters act as individual cells in series, which significantly reduce their overall resistances to flow. Because of the timescales at which clusters unfold to enter constrictions and reorganize after exiting (approximately milliseconds to seconds), the responses of CTC clusters are likely dominated by the state of existing intercellular adhesions and cytoskeletal elements. An interesting area of investigation is whether the physical forces exerted on clusters during transit may contribute to the greater metastatic ability of CTC clusters vs. singlets (6–9). For example, mechanotransduction pathways involved in the metastatic progression of cancer cells (39, 40) may provide CTC clusters with biophysical cues that promote the extravasation, migration, and eventual colonization of new tumors.

Finally, strategies that interfere with cell–cell or cell–matrix adhesions may lead to the disruption of clusters in constrictions where high intravascular shear forces are present. Because of the greater metastatic potential of clustered circulating tumor cells than singlets (9) and of larger clusters vs. smaller clusters (7), this strategy may be an effective method of reducing the probability of metastasis, the leading cause of cancer mortality worldwide.

## Materials and Methods

Single CTCs and CTC clusters containing ~2–20 cells of patient (obtained with informed consent according to Massachusetts General Hospital Institutional Review Board Protocol 05-300) and cancer cell line origins were introduced into 5- to 10-μm microfluidic constrictions under pressure drops of 7–83 cm $H_2O$ at 37 °C and analyzed using custom Matlab scripts to calculate cell/nuclear sizes (Fig. S10) and velocities. Human cultured CTC clusters were introduced into the bloodstream of 3 d postfertilization *Tg(kdrl:mCherry)* transgenic zebrafish (Massachusetts General Hospital Subcommittee on Research Animal Care Protocol 2011N000127) for observation. Complete materials and methods are available in *Supporting Information*.

**ACKNOWLEDGMENTS.** We thank E. Reategui, X. Hong, S. Pan, D. Miyamoto, N. V. Jordan, M. Choz, M. Zeinali, R. Oklu, T. Todorova, and L. Sequist for helping with patient sample acquisition, coordination, and processing. We are grateful to A. Khankhel and A. Chandrasekaran for microfabrication of masters; C. Angpraseuth, R. Desai, and R. O'Keefe for device fabrication; and X. Jiang, A. Stoddard, J. Edd, F. Ellett, S. Angione, N. Aceto, L. Libby, and C. Mackenzie for helpful discussions. We are indebted to O. Hurtado for microfabrication guidance. This work was financially supported by NIH Grant F33-GM109574 (to B.D.S.), Howard Hughes Medical Institute (D.A.H.), Alex Lemonade Stand Foundation (D.M.L.), Live Like Bella Foundation (D.M.L.), NIH Grant R24OD016761 (to D.M.L.), NIH Grant P41 EB002503-11 (to M.T.), and NIH National Institute of Biomedical Imaging and Bioengineering Quantum Grant (to M.T. and D.A.H.).

1. Yu M, Stott S, Toner M, Maheswaran S, Haber DA (2011) Circulating tumor cells: Approaches to isolation and characterization. *J Cell Biol* 192(3):373–382.
2. Hong B, Zu Y (2013) Detecting circulating tumor cells: Current challenges and new trends. *Theranostics* 3(6):377–394.
3. Krebs MG, et al. (2014) Molecular analysis of circulating tumour cells—biology and biomarkers. *Nat Rev Clin Oncol* 11(3):129–144.
4. Paterlini-Brechot P, Benali NL (2007) Circulating tumor cells (CTC) detection: Clinical impact and future directions. *Cancer Lett* 253(2):180–204.
5. Hou JM, et al. (2012) Clinical significance and molecular characteristics of circulating tumor cells and circulating tumor microemboli in patients with small-cell lung cancer. *J Clin Oncol* 30(5):525–532.
6. Fidler IJ (1973) The relationship of embolic homogeneity, number, size and viability to the incidence of experimental metastasis. *Eur J Cancer* 9(3):223–227.
7. Liotta LA, Saidel MG, Kleinerman J (1976) The significance of hematogenous tumor cell clumps in the metastatic process. *Cancer Res* 36(3):889–894.
8. Fidler IJ (1978) Tumor heterogeneity and the biology of cancer invasion and metastasis. *Cancer Res* 38(9):2651–2660.
9. Aceto N, et al. (2014) Circulating tumor cell clusters are oligoclonal precursors of breast cancer metastasis. *Cell* 158(5):1110–1122.
10. Hou JM, et al. (2011) Circulating tumor cells as a window on metastasis biology in lung cancer. *Am J Pathol* 178(3):989–996.
11. Yu M, et al. (2013) Circulating breast tumor cells exhibit dynamic changes in epithelial and mesenchymal composition. *Science* 339(6119):580–584.
12. Balzer EM, Konstantopoulos K (2012) Intercellular adhesion: Mechanisms for growth and metastasis of epithelial cancers. *Wiley Interdiscip Rev Syst Biol Med* 4(2):171–181.
13. Carlsson A, et al. (2014) Circulating tumor microemboli diagnostics for patients with non-small-cell lung cancer. *J Thorac Oncol* 9(8):1111–1119.
14. Yu M, et al. (2014) Cancer therapy. Ex vivo culture of circulating breast tumor cells for individualized testing of drug susceptibility. *Science* 345(6193):216–220.
15. Chaffer CL, Weinberg RA (2011) A perspective on cancer cell metastasis. *Science* 331(6024):1559–1564.
16. Weiss L (1987) The hemodynamic destruction of circulating cancer cells. *Biorheology* 24(2):105–115.
17. Molnar B, Ladanyi A, Tanko L, Sréter L, Tulassay Z (2001) Circulating tumor cell clusters in the peripheral blood of colorectal cancer patients. *Clin Cancer Res* 7(12):4080–4085.
18. Cho EH, et al. (2012) Characterization of circulating tumor cell aggregates identified in patients with epithelial tumors. *Phys Biol* 9(1):016001.
19. Hou JM, et al. (2011) Molecular features and clinical relevance of circulating tumor cells (CTC) and circulating tumor microemboli (CTM) in patients with small cell lung cancer (SCLC). *Clin Exp Metastasis* 28(2):221–222.
20. Zeidman I, Buss JM (1952) Transpulmonary passage of tumor cell emboli. *Cancer Res* 12(10):731–733.
21. Fung YC, Zweifach BW, Intaglietta M (1966) Elastic environment of the capillary bed. *Circ Res* 19(2):441–461.
22. Baskurt OK, Meiselman HJ (2003) Blood rheology and hemodynamics. *Semin Thromb Hemost* 29(5):435–450.
23. Byun S, et al. (2013) Characterizing deformability and surface friction of cancer cells. *Proc Natl Acad Sci USA* 110(19):7580–7585.
24. Bathe M, Shirai A, Doerschuk CM, Kamm RD (2002) Neutrophil transit times through pulmonary capillaries: The effects of capillary geometry and fMLP-stimulation. *Biophys J* 83(4):1917–1933.
25. Davidson PM, Denais C, Bakshi MC, Lammerding J (2014) Nuclear deformability constitutes a rate-limiting step during cell migration in 3-D environments. *Cell Mol Bioeng* 7(3):293–306.
26. Harada T, et al. (2014) Nuclear lamin stiffness is a barrier to 3D migration, but softness can limit survival. *J Cell Biol* 204(5):669–682.
27. Chen J, et al. (2011) Classification of cell types using a microfluidic device for mechanical and electrical measurement on single cells. *Lab Chip* 11(18):3174–3181.
28. King MR, et al. (2015) A physical sciences network characterization of circulating tumor cell aggregate transport. *Am J Physiol Cell Physiol* 308(10):C792–C802.
29. Williams SA, et al. (1988) Dynamic measurement of human capillary blood pressure. *Clin Sci (Lond)* 74(5):507–512.
30. Sarioglu AF, et al. (2015) A microfluidic device for label-free, physical capture of circulating tumor cell clusters. *Nat Methods* 12(7):685–691.
31. Chen Y-L (2014) Inertia- and deformation-driven migration of a soft particle in confined shear and Poiseuille flow. *RSC Advances* 4(34):17908–17916.
32. Maître JL, et al. (2012) Adhesion functions in cell sorting by mechanically coupling the cortices of adhering cells. *Science* 338(6104):253–256.
33. Duguay D, Foty RA, Steinberg MS (2003) Cadherin-mediated cell adhesion and tissue segregation: Qualitative and quantitative determinants. *Dev Biol* 253(2):309–323.
34. Golubovskaya VM, et al. (2008) A small molecule inhibitor, 1,2,4,5-benzenetetraamine tetrahydrochloride, targeting the Y397 site of focal adhesion kinase decreases tumor growth. *J Med Chem* 51(23):7405–7416.
35. Ling Y, Zhong Y, Perez-Soler R (2001) Disruption of cell adhesion and caspase-mediated proteolysis of beta- and gamma-catenins and APC protein in paclitaxel-induced apoptosis. *Mol Pharmacol* 59(3):593–603.
36. Isogai S, Horiguchi M, Weinstein BM (2001) The vascular anatomy of the developing zebrafish: An atlas of embryonic and early larval development. *Dev Biol* 230(2):278–301.
37. Sasportas LS, Gambhir SS (2014) Imaging circulating tumor cells in freely moving awake small animals using a miniaturized intravital microscope. *PLoS One* 9(1):e86759.
38. Hu N, Sedmera D, Yost HJ, Clark EB (2000) Structure and function of the developing zebrafish heart. *Anat Rec* 260(2):148–157.
39. Stroka KM, Konstantopoulos K (2014) Physical biology in cancer. 4. Physical cues guide tumor cell adhesion and migration. *Am J Physiol Cell Physiol* 306(2):C98–C109.
40. Jaalouk DE, Lammerding J (2009) Mechanotransduction gone awry. *Nat Rev Mol Cell Biol* 10(1):63–73.
41. Stott SL, et al. (2010) Isolation of circulating tumor cells using a microvortex-generating herringbone-chip. *Proc Natl Acad Sci USA* 107(43):18392–18397.
42. Abdelgawad M, et al. (2011) A fast and simple method to fabricate circular microchannels in polydimethylsiloxane (PDMS). *Lab Chip* 11(3):545–551.
43. Fiddes LK, et al. (2010) A circular cross-section PDMS microfluidics system for replication of cardiovascular flow conditions. *Biomaterials* 31(13):3459–3464.
44. Wang Y, et al. (2010) Moesin1 and Ve-cadherin are required in endothelial cells during in vivo tubulogenesis. *Development* 137(18):3119–3128.
45. Hsu CW, Chen YL (2010) Migration and fractionation of deformable particles in microchannel. *J Chem Phys* 133(3):034906.
46. Skalak R, Branemark PI (1969) Deformation of red blood cells in capillaries. *Science* 164(3880):717–719.
47. Batchelor GK (1967) *An Introduction to Fluid Dynamics* (Cambridge Univ Press, Cambridge, UK).
48. Lighthill MJ (1968) Pressure-forcing of tightly fitting pellets along fluid-filled elastic tubes. *J Fluid Mech* 34(1):113–143.
49. Zhang Z, Xu J, Hong B, Chen X (2014) The effects of 3D channel geometry on CTC passing pressure—towards deformability-based cancer cell separation. *Lab Chip* 14(14):2576–2584.